

## Compression Behavior of Biodegradable Thermoplastic Plasticizer-Containing Composites

A. F. Guo,<sup>a,1</sup> J. F. Li,<sup>b</sup> F. Y. Li,<sup>b</sup> J. Xu,<sup>b</sup> C. W. Zhang,<sup>b</sup> and S. Chen<sup>b</sup>

<sup>a</sup> School of Mechanical & Automobile Engineering, Liaocheng University, Liaocheng, China

<sup>b</sup> School of Mechanical Engineering, Shandong University, Jinan, China

<sup>1</sup> guoanfu@lcu.edu.cn

*Thermoplastic starch-based composites generate worldwide interest as they are based on green raw materials and undergo complete degradation. The composites were first fabricated from starch and sisal fibers as the major materials via the forming process. The effect of starches with different contents of single- and multicomponent plasticizers on the cushioning properties of the composites was studied. An increase in plasticizer contents within a certain range is shown to enhance materials resistance to pressure and its cushioning performance. With the multicomponent plasticizer content of 15%, the resistance to pressure for four types of composites prepared at different weight ratios of formamide and urea were of the order of 2:1>1:1>1:2, and that of the four types of composites fabricated at different weight ratios of glycerol and ethylene glycol were of the order of 1:2>2:1>1:1. Multicomponent plasticizer-containing starch-based composites are shown to be irregular elastomers and the stress-strain relation to be first defined by a hyperbolic tangent curve function and then by the tangent one.*

**Keywords:** biodegradation, starch-based composite, single/multicomponent plasticizers, cushioning package, compression behavior.

**Introduction.** The application of plastic packing materials has brought considerable convenience to humansociety, but also leads to “white pollution” and other environmental problems. To solve these problems, scholars [1–4] have focused on the use of biomass composites in recent decades. Starch-based composites are a class of new cushion packaging materials whose principal components are plant fibers and starch. Starch-based composites using natural resources as raw materials possess excellent biodegradability [5–8]. These composites can not only mitigate the pollution problem but also avert a biochemical crisis [9–11]. Therefore, green alternatives such as starch-based composites are presently a hot topic of research.

Starch is a natural polymer with many intramolecular and intermolecular hydrogen bonds; hence, its molecules are strongly bonded. When small molecules are added into starch and mixed, new hydrogen bonds are formed that are capable of replacing the hydrogen bonds of starch molecules. The new hydrogen bonds can decrease the intermolecular force of molecules and increase their capacity for action [12, 13]. Thus, these small molecules impart thermoplasticity to plastic. As an important component of starch-based composites, thermoplastic starch (TPS) significantly influences the properties of the compound material.

In recent years, many reports have been published on TPS-based composites. Liu et al. [14] studied the plasticizing mechanism of plasticized starch by infrared spectroscopy and X-ray diffraction. Ma and Yu [15, 16] studied the mechanism of interaction between the hydrogen bonds of starch and the plasticizer in glycerol-plasticized thermoplastic starch (GPTPS) and formamide-plasticized thermoplastic starch (FPTPS). Aichholzer and Fritz [17] and Della Valle et al. [18] analyzed the rheological properties of TPS-based composites. Guo et al. [19] and Canché-Escamilla et al. [20] studied the biodegradability of TPS composites. Some scholars [21–24] investigated the cushioning performance of

common cushion packaging materials using static compression tests. Nevertheless, to the best of the authors' knowledge, there has been no comprehensive study focusing on the mechanical properties of TPS-based composites.

In this study, the effect of TPS with different proportions of single and compound plasticizers on the cushioning properties of their composites was studied by analyzing the static compression curves of the composites via static compression tests using formamide, urea, glycerol, and ethylene glycol as plasticizers.

### 1. Materials and Experiments.

**1.1. Materials and Equipment.** Materials: Sisal fibers of 100–150 mesh with a length of 5–10 mm were provided by Yantai Jiulong Co., Ltd. Corn starch with an average diameter of 70 nm was purchased from Hebei Huachen Starch Sugar Co., Ltd. Analytical reagent (AR) grade formamide was purchased from Tianjin Damao Chemical Reagent Factory. AR grade urea was purchased from Tianjin Guangcheng Chemical Reagent Co., Ltd. AR grade ethylene glycol and glycerol were purchased from Tianjin Fuyu Fine Chemical Co., Ltd. Other materials such as talcum powder of 0.038 mm grade, stearic acid, foaming agent AC, polyvinyl alcohol (99% purity) AR grade sodium hydroxide, and distilled water were purchased from Tianjin Guangcheng Chemical Reagent Co., Ltd. Table 1 shows the materials used in the preparation.

Table 1

Materials Used in the Preparation

Material	Type	Material	Type	Material	Type
Sisal fiber	5–10 mm length	Urea	AR grade	Talcum powder	0.038 mm grade
Corn starch	70 nm diameter	Ethylene glycol	AR grade	Polyvinyl alcohol	99% purity
Formamide	AR grade	Glycerol	AR grade	Sodium hydroxide	AR grade

Testing equipment included: electronic constant temperature water bath (model HHS-2), precision electric mixer (model JJ-1), electronic balance (model JM-B), electrothermal constant temperature dry box (model DHG), double column simplex mechanical compression machine, and microcomputer-controlled electron universal testing machine (model WDW-100A).

**1.2. Preparation of Starch-Based Composite.** The preparation process can be subdivided into four stages: fiber pre-treatment, TPS preparation, slurry mixture, and foaming (Fig. 1).

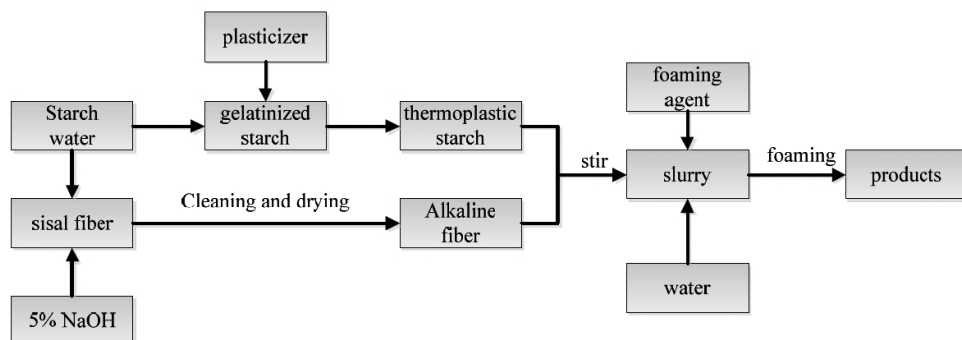


Fig. 1. Preparation of thermoplastic starch-based composites.

(1) Fiber pretreatment: The sisal fibers were immersed in 5% sodium hydroxide solution for 4 h. Then, they were washed with distilled water until pH=7 was reached. Finally, they were dried at 80°C for 8 h in a heat oven.

(2) TPS preparation: Single plasticizer: FPTPS and urea plasticized thermoplastic starch (UPTPS) were compounded in the proportion of 10, 15, and 20%. GPTPS and ethylene glycol-plasticized thermoplastic starch (EGPTPS) were compounded in the proportion of 15%.

Compound plasticizer: The proportion of formamide to urea in formamide-urea plasticized thermoplastic starch (FUPTPS) was set at 2:1, 1:2, and 1:1. The proportion of glycerol to ethylene glycol in glycerol-ethylene glycol-plasticized thermoplastic starch (GGPTPS) was set at 2:1, 1:2, and 1:1.

Starch and water were mixed according to the formula ratio. Then starch was pasted in 75-85°C water. Subsequently, the plasticizer was stirred and added to the starch.

(3) Slurry mixture: The amount of TPS and sisal fibers used in this process was 500 g. They were treated by alkali, added to a mixer, and stirred for 20 min at room temperature. Subsequently, the additives were added to the slurry for 30 min.

(4) Foaming: The mixed slurry was poured into a mold of size 300×300 mm, with the upper mold temperature set at 180°C, the lower mold temperature set at 195°C, pressure set at 3 MPa, and the elevate pressure was set of 20 s. Then, the pressure process was continued for 30 s. Finally, the product was removed from the mold.

**1.3. Testing of Mechanical Properties of Starch-Based Composite.** According to the method of GB 8168-2008 [25], standard samples (100×100×25 mm) were used for the static compression test. The samples were pressed by increasing load along the width at a speed of 12 mm/min. The test was performed at a speed of 10 mm/min until the sample was crushed. The loads were recorded automatically. The compressive stress and strain were calculated by formulas (1) and (2), respectively:

$$\sigma = \frac{P}{A}, \quad (1)$$

where  $\sigma$  is the compressive stress (MPa),  $P$  is compressive load (N), and  $A$  is test sample cross-sectional area ( $\text{mm}^2$ ),

$$\varepsilon = \frac{T - T_j}{T}, \quad (2)$$

where  $\varepsilon$  is the compressive strain (%),  $T$  is original thickness of testing sample (mm), and  $T_j$  is thickness after testing (mm).

According to the stress-strain curve obtained by analyzing the test data, the volume deformation energy and cushion coefficient at different stresses were calculated. Then, the cushion coefficient-stress curve was plotted as follows:

(i) Divide the area under the stress-strain curve into several small areas. The smaller the area, the higher is the computational accuracy.

(ii) Calculate  $\sigma_i$  and  $\varepsilon_i$  ( $i = 1, 2, 3, \dots$ ).

(iii) Calculate the increment in every stressed section, that is, calculate the proportion of each area

$$\Delta u_i = \frac{1}{2}(\sigma_i + \sigma_{i-1})(\varepsilon_i - \varepsilon_{i-1}). \quad (3)$$

(iv) Calculate the corresponding creep resistance  $u_i$ ,

$$u_i = \sum \Delta u_k \quad (k = 1, 2, \dots, i). \quad (4)$$

(v) Calculate the corresponding cushion coefficient  $C_i$ ,

$$C_i = \frac{\sigma_i}{u_i}. \quad (5)$$

(vi) Draw the cushion coefficient–maximum stress curve, taking  $C$  as the ordinate and  $\sigma$  as the abscissa.

## 2. Results and Discussion.

**2.1. Influence of Single Plasticizers on Properties of Composites.** Figure 2 shows the compressive stress–strain curves of the FPTPS- and UPTPS-based composites, respectively. When the plasticizer content is in the range 10–20% at a fixed strain, the stress decreases with an increase in the plasticizer content. The higher the resistance to pressure of the material, the greater its cushioning performance.

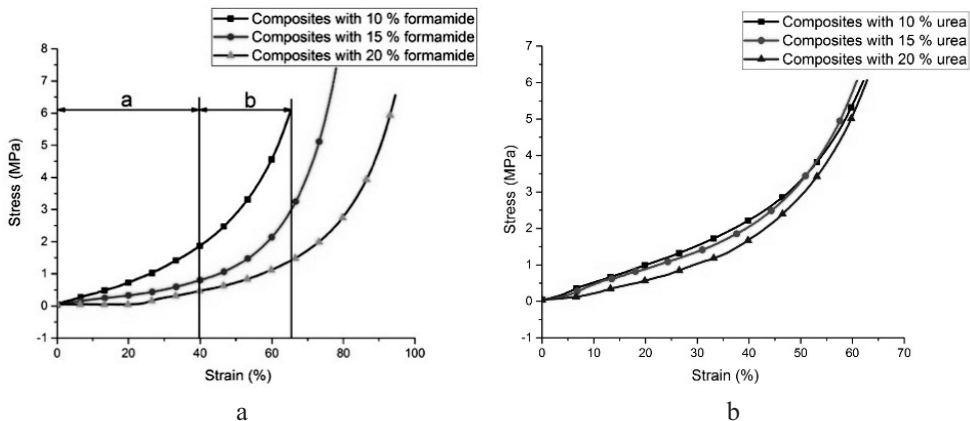


Fig. 2. Compressive stress–strain curves of FPTPS- (a) and UPTPS-based (b) composites.

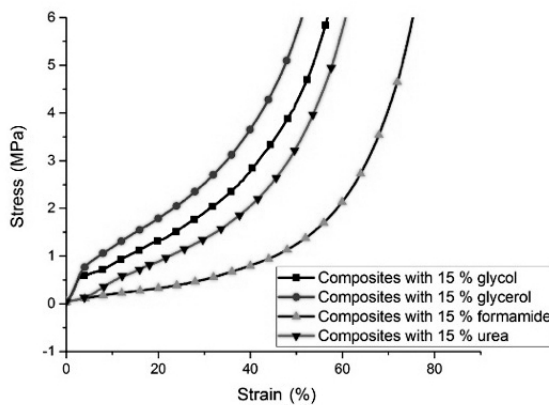


Fig. 3. Compressive stress–strain curves of four starch-based composites.

Figure 3 shows the compressive stress–strain curves of the GPTPS-, EGPTPS-, UPTPS-, and FPTPS-based composites with a plasticizer content of 15%. When the plasticizer content is fixed, the stress of the four materials follows the order FPTPS < UPTPS < EGPTPS < GPTPS; therefore, the resistance to pressure follows the order FPTPS > UPTPS > EGPTPS > GPTPS. As stated above, the higher the resistance to pressure, the better the cushioning performance. Accordingly, the cushioning performance

of FPTPS and UPTPS is better than that of EGPTPS and GPTPS. The reason for the higher stress of FPTPS and UPTPS is that formamide and urea have a C=O group and exhibit strong electronegativity; hence, they easily form hydrogen bonds with the hydrogen atoms of starch. Besides, the  $-NH_2$  group of formamide and urea can form hydrogen bonds with the ether bonds of starch. Therefore, the plasticizing effect of formamide and urea is better than that of glycerol and ethylene glycol; thus, better-quality TPS can be obtained when using formamide and urea as plasticizers.

As shown in Fig. 2, FPTPS and UPTPS are tangent-curve elastomers that show a kind of tangential relation between stress and strain. Taking the stress-strain curve of UPTPS with a plasticizer content of 10% as an example, in segment *a*, strain increases gradually with increasing stress, the local distortion of stress is larger, and stress does not exhibit a very large change; hence, the material shows definite cushioning performance. In segment *b*, when stress reaches the extreme value of compression, bubbles in the material burst and gas is expelled, and the material is pressed. Therefore, the stress increases sharply and the cushioning effect disappears.

Figure 4a shows the static cushion coefficient-stress curves of the FPTPS-based composites. Figure 4b shows the static cushion coefficient-stress curves of the UPTPS-based composites. As can be seen from Fig. 4a, the cushion coefficient of the material first decreases and then stabilizes with an increase in stress; the smallest cushion coefficient obtained for the FPTPS-based composites is 5. Figure 4b also shows that the cushion coefficient of the material decreases first and then stabilizes with an increase in stress; the smallest cushion coefficient obtained for the UPTPS-based composites is in the range 4–6.

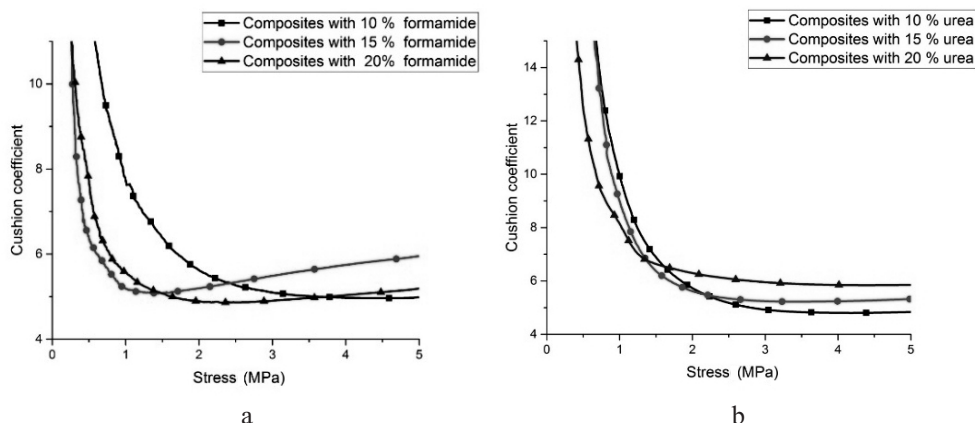


Fig. 4. Static cushion coefficient-stress curves of FPTPS- (a) and UPTPS-based (b) composites.

**2.2. Influence of Compound Plasticizers on Properties of Composites.** Figure 5a shows the compressive stress-strain curves of FUPTPS-based composites. At a plasticizer content of 15%, the resistance to pressure of the starch-based composites prepared using different mass ratios of formamide and urea follows the order 2:1 > 1:1 > 1:2. Figure 2b shows that the cushioning performance of the FPTPS-based composites is better than that of the UPTPS-based composites, with the latter being hard and brittle. If urea is replaced by formamide, the brittleness of the compound material decreases, increasing its flexibility.

Figure 5b shows the compressive stress-strain curves of the GGPTPS-based composites. At a plasticizer content of 15%, the resistance to pressure of the starch-based composites prepared using different mass ratios of glycerol and ethylene glycol follows the order 2:1 > 1:1 > 1:2. Figure 3 shows that the cushioning performance of the EGPTPS-based composites is better than that of the GPTPS-based composites. Similarly, when

glycerol is partially replaced by ethylene glycol, the cushioning performance of the compound material is enhanced.

Under conditions of constant compound plasticizer content and stress, the mass ratio of the compound plasticizer and resistance to pressure are different.

From Fig. 5, we can see that FUPTPS and GGPTPS are irregular elastomers. Their stress-strain relation first shows a hyperbolic tangent curve function and then a tangent curve function. Taking compressive stress-strain curves of FUPTPS-based composites in Fig. 5a as an example, we can see a hyperbolic tangent curve function relationship in segment *c*, and at the elastic stage, the material undergoes a small deformation and the cushioning performance is good. However, there exists a tangent curve function relationship in segments *d* and *e*.

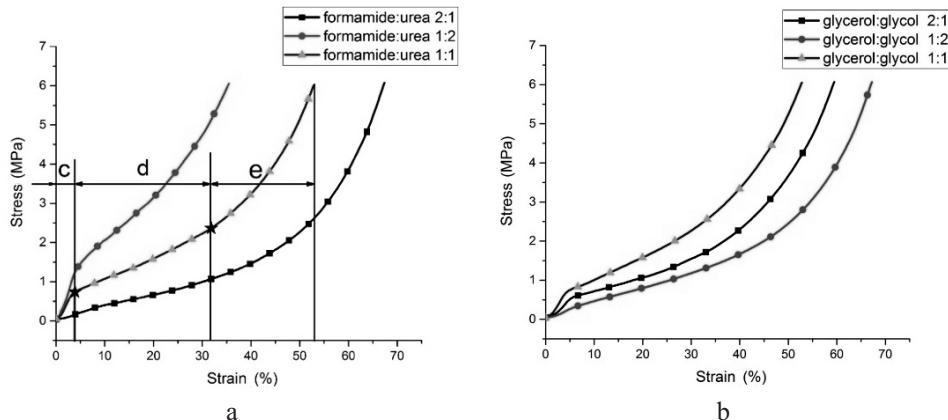


Fig. 5. Compressive stress-strain curves of FUPTPS- (a) and GGPTPS-based (b) composites.

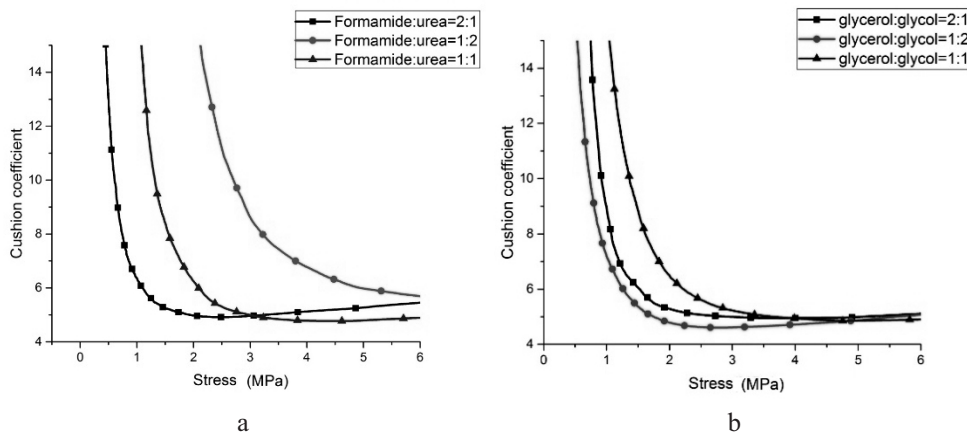


Fig. 6. Static cushion coefficient-stress curves of FUPTPS- (a) and GGPTPS-based (b) composites.

Figure 6a shows the static cushion coefficient-stress curves of the FUPTPS-based composites. With increasing stress, the cushion coefficient of the material first decreases and then stabilizes. The smallest cushion coefficient obtained for the FUPTPS-based composites is between 4.5 and 5.5. With a change in the mass ratio of formamide and urea, the cushion coefficient of the material changes greatly. When the mass ratio of formamide and urea in the compound plasticizer is 2:1, the cushion coefficient is the smallest and the cushioning performance of the material is the best.

Figure 6b shows the static cushion coefficient–stress curves of the GGTPS-based composites. We can see that with increasing stress, the cushion coefficient of the material first decreases and then stabilizes. The smallest cushion coefficient for the GGTPS-based composites is between 4.5 and 5. With a change in the mass ratio of glycerol and ethylene glycol, the cushion coefficient of the material changes greatly. When the mass ratio of glycerol and ethylene glycol in the compound plasticizer is 1:2, the cushion coefficient is the smallest and the cushioning performance of the material is the best.

## Conclusions

1. Plasticizers enhance the flexibility of starch-based composites. Within a certain range, as the plasticizer content increases, the resistance to pressure of the composite and its cushioning performance increase.

2. FPTPS and UPTPS are tangent-curve elastomers showing a kind of tangential relation between stress and strain, while compound plasticizer starch-based composite materials are irregular elastomers. The stress-strain relation of the latter is first a hyperbolic tangent curve function and then a tangent curve function.

3. When the single plasticizer content is 15%, the resistance to pressure of the four types of composites prepared using single plasticizers follows the order FPTPS > UPTPS > EGTPS > GPTPS. When the compound plasticizer content is 15%, the resistance to pressure of the four types of FUPTPS composites prepared using different mass ratios of formamide and urea follows the order 2:1 > 1:1 > 1:2, and that of the four types of GGTPS composites prepared using different mass ratios of glycerol and ethylene glycol follows the order 1:2 > 2:1 > 1:1.

**Acknowledgments.** The authors gratefully appreciate the financial support from the National Natural Science Foundation of China (Nos. 51775318, 51305239, and 51275278), and Natural Science Foundation of Shandong Provincial (Nos. ZR2013EEQ010 and 2014ZRB019XH). We also appreciate the assistance of our colleagues from Shandong University, China.

1. W. W. Hu, X. H. Yu, Q. Hu, et al., “Methyl orange removal by a novel PEI-AuNPs-hemin nanocomposite,” *J. Environ. Sci.*, **53**, 278–283 (2017).
2. C. Y. Sun, Q. H. Xu, Y. Xie, et al., “High-efficient one-pot synthesis of carbon quantum dots decorating Bi<sub>2</sub>MoO<sub>6</sub> nanosheets heterostructure with enhanced visible-light photocatalytic properties,” *J. Alloy. Compd.*, **723**, 333–344 (2017).
3. Q. L. Yue, Y. N. Hou, S. Z. Yue, et al., “Construction of an off-on fluorescence system based on carbon dots for trace pyrophosphate sensing,” *J. Fluoresc.*, **25**, 585–594 (2015).
4. Q. L. Yue, T. F. Shen, L. Wang, et al., “A convenient sandwich assay of thrombin in biological media using nanoparticle-enhanced fluorescence polarization,” *Biosens. Bioelectron.*, **56**, 231–236 (2014).
5. Z. F. Jia, H. Q. Li, Y. Zhao, et al., “Preparation and electrical properties of sintered copper powder compacts modified by polydopamine-derived carbon nanofilms,” *J. Mater. Sci.*, **53**, No. 9, 6562–6573 (2018).
6. C. H. Song, M. X. Li, H. Qi, et al., “Impact of anti-acidification microbial consortium on carbohydrate metabolism of key microbes during food waste composting,” *Bioresource Technol.*, **259**, 1–9 (2018).
7. J. Gironès, E. F. X. Espinach, N. Pellicer, et al., “High-performance-tensile-strength alpha-grass reinforced starch-based fully biodegradable composites,” *Bioresources*, **8**, No. 4, 6121–6135 (2013).

8. J. L. Guimarães, F. Wypych, C. K. Saul, et al., "Studies of the processing and characterization of corn starch and its composites with banana and sugarcane fibers from Brazil," *Carbohyd. Polym.*, **80**, No. 1, 130–138 (2010).
9. H. P. S. Abdul Khalil, A. H. Bhat, and A. F. Ireneana Yusra, "Green composites from sustainable cellulose nanofibrils: A review," *Carbohyd. Polym.*, **87**, No. 2, 963–979 (2012).
10. S. Chen, Q. Ji, L. Q. Kong, et al., "The electrochromic properties of an alternative copolymer containing benzo[1,2-b:4,5-b'] dithiophene as the electron donor and benzoselenadiazole as the electron acceptor units," *Int. J. Electrochem. Sci.*, **12**, No. 4, 3398–3416 (2017).
11. C. W. Zhang, F. Y. Li, J. F. Li, et al., "Research on rheological behavior of biobased composite slurry composed of sisal fiber and thermoplastic oxidized starch," *J. Biobased. Mater. Bio.*, **11**, No. 2, 119–124 (2017).
12. X. Zhang, X. L. Wang, Q. L. Wang, et al., "Hydride ion ( $H^-$ ) transport behavior in barium hydride under high pressure," *Phys. Chem. Chem. Phys.*, **20**, No. 13, 8917–8923 (2018).
13. Y. Z. Wan, H. Luo, F. He, et al., "Mechanical, moisture absorption, and biodegradation behaviours of bacterial cellulose fibre-reinforced starch biocomposites," *Compos. Sci. Technol.*, **69**, Nos. 7–8, 1212–1217 (2009).
14. P. Liu, F. Y. Li, J. F. Li, et al., "Thermoplastic starch matrix plasticized by single/compound plasticizer in starch-based composites," *Adv. Funct. Mater.*, **45**, No. 14, 14140–14144 (2014).
15. X. F. Ma and J. G. Yu, "Thermoplastic starch plasticized by the mixture of urea and formamide," *Acta Polym. Sin.*, No. 4, 483–489 (2004).
16. X. F. Ma and J. G. Yu, "Hydrogen bond of thermoplastic starch and effects on its properties," *Acta Chim. Sinica*, **62**, No. 12, 1180–1184 (2004).
17. W. Aichholzer and H.-G. Fritz, "Rheological characterization of thermoplastic starch materials," *Starch-Starke*, **50**, No. 50, 77–83 (1998).
18. G. Della Valle, B. Vergnes, and D. Lourdin, "Viscous properties of thermoplastic starches from different botanical origin," *Int. Polym. Proc.*, **22**, No. 5, 471–479 (2007).
19. A. F. Guo, J. F. Li, F. Y. Li, and B. K. Wei, "Study on the biodegradability of plant fiber and starch dishware," *J. Funct. Mater.*, **40**, No. 11, 1929–1932 (2009).
20. G. Canché-Escamilla, M. Canché-Canché, S. Duarte-Aranda, et al., "Mechanical properties and biodegradation of thermoplastic starches obtained from grafted starches with acrylics," *Carbohyd. Polym.*, **86**, No. 4, 1501–1508 (2011).
21. T. Ma, Y. L. Wang, J. Wan, and L. W. Zhang, "Common cushion packing materials static compress property testing study," *Packaging Eng.*, **23**, No. 2, 4–8 (2002).
22. B. L. Lu, "Research on static compression cushion curve of EPE polyethylene foaming material," *Packaging Eng.*, **28**, No. 2, 42–44 (2007).
23. X. Ming, Y. Zhao, J. Lu, and Q. L. Peng, "Contrast and analysis of packaging material cushioning performance based on static compression testing," *Packaging Eng.*, **27**, No. 2, 59–61 (2006).
24. A. Guo, J. Zhao, J. Li, and K. Guan, "Forming parameters optimisation of biomass cushion packaging material by orthogonal test," *Mater. Res. Innov.*, **19**, S5-521–S5-525 (2015).
25. GB/T 8168-2008. *Testing Method of Static Compression for Packaging Cushioning Materials.*

Received 15. 03. 2018